IMPROVED GRAPH-BASED USER SCHEDULING FOR SUM-RATE MAXIMIZATION IN LEO-NTN SYSTEMS

Bilal Ahmad ⋆, Daniel Gaetano Riviello⋆, Alessandro Guidotti †, Alessandro Vanelli-Coralli ⋆.

Department of Electrical, Electronic, and Information Engineering (DEI), University of Bologna ⋆
National Inter-University Consortium for Telecommunications (CNIT), Bologna, Italy †
{bilal.ahmad6, daniel.riviello, a.guidotti, alessandro.vanelli}@unibo.it

ABSTRACT

In this paper, we study the problem of user scheduling for Low Earth Orbit (LEO) Multi-User (MU) Multiple-Input-Multiple-Output (MIMO) Non-Terrestrial Network (NTN) systems with the objective of maximizing the sum-rate capacity while minimizing the total number of clusters. We propose an iterative graph-based maximum clique scheduling approach with constant graph density. Users are grouped together based on the channel coefficient of correlation (CoC) as dissimilarity metric and served by the satellite via Space Division Multiple Access (SDMA) by means of Minimum Mean Square Error (MMSE) digital beamforming on a cluster basis. Clusters are then served in different time slots via Time Division Multiple Access (TDMA). The results, presented in terms of per-cluster sum-rate capacity and per-user throughput, show that the presented approach can significantly improve the system performance.

Index Terms— LEO, MU-MIMO, User Scheduling, Beamforming, MMSE

1. INTRODUCTION

With the approval of 3GPP Rel-17 and the inclusion of Non-Terrestrial Networks (NTN) in 5G-Advanced and 6G systems, the satellite industry is undergoing a rapid growth, paving the way for global access to 6G services. Specifically, NTNs in Low Earth Orbit (LEO) have revealed their potential as they provide high data rates with lower latency and better link budget [1]. To further increase the data rate, aggressive (full) frequency reuse schemes provide a more effective use of the bandwidth, thus improving the spectral efficiency, at the cost of an increased interference that must be managed at the receiver via Multi-User Detection (MUD) and/or transmitter via precoding/beamforming, [2].

Although precoding techniques can improve the performance, there must be a trade-off between computational complexity and performance reduction. For example, Dirty Paper Coding (DPC) achieves the channel capacity, but due to its high computational complexity, it is still not widely used in existing practical systems [3]. Thanks to lower computational costs and close to the ideal performance, linear precoding and detection schemes, such as Zero Forcing (ZF), MMSE or Signal-to-Leakage-plus-Noise Ratio (SLNR) beamforming [4, 5], are more desirable in NTN MU-MIMO systems as compared to non-linear precoding [6]. A thorough survey on MIMO techniques applied to SatCom is provided in [7], where both fixed and mobile satellite systems are evaluated and the main channel impairments are addressed.

Conceptually, adding more antennas at the satellite increases the system capacity, thus enhancing energy efficiency and significantly boosting the system throughput [8]. Designing algorithms that can address the issue of scarce system resources in the MU-MIMO LEO system is therefore a fundamental, and challenging, technology for NTN. Since the number of User Terminals (UTs) on the ground is much larger than the on-board satellite antennas, efficient user scheduling is required. Scheduling can be accomplished by grouping users into different clusters: i) UTs within the same cluster are multiplexed and served together via Space Division Multiple Access (SDMA), i.e., digital beamforming or Multi-User MIMO (MU-MIMO) techniques; and ii) the different clusters are then served on different time slots via Time Division Multiple Access (TDMA) [9, 10, 11]. The design of an optimal user grouping strategy is known to be an NP-complete problem which can be solved only through exhaustive search [12]. A greedy user scheduling strategy for downlink MU-MIMO, which takes into account heterogeneous users, has been proposed in [10]. Multiple antenna downlink orthogonal clustering (MADOC), a well-established low-complexity algorithm introduced in [11], builds on the previous work by taking user fairness and group number minimization into account.

In this paper, we extend our previous work in [9] by proposing a low-complexity graph-based iterative procedure with constant graph density for user scheduling in MU-MIMO LEO NTN systems and we aim at maximizing the sum-rate capacity while preserving fairness among the users.

Part of this work has been funded by the 6G-NTN project, which received funding from the Smart Networks and Services Joint Undertaking (SNS JU) under the European Union's Horizon Europe research and innovation programme under Grant Agreement No 101096479.

We model the clustering problem as an undirected and unweighted graph and we iteratively search for the maximum clique, i.e., the largest fully connected subgraph to form clusters of spatially separable users. We perform an heuristic optimization, i.e., via exhaustive simulations, of the graph density value, which maximizes the sum-rate capacity. We show that the proposed approach can significantly improve the performance w.r.t. our previous work [9] and MADOC.

2. SYSTEM MODEL

We focus on the downlink of a single LEO satellite operating in S-band equipped with an antenna array. The array consists of N radiating elements which provide connectivity to K uniformly distributed on-ground single-antenna users under the assumption that $N \ll K$. Our additional assumptions are based on the system architecture, which is thoroughly described in [1, 9, 13]. In particular, we consider non-ideal Channel State Information (CSI) with channel aging, i.e., we take into account the latency Δt between the channel estimation time and the transmission time, which introduces a misalignment between the channel on which the scheduling and beamforming matrices are generated and the actual channel through which the transmission occurs [9, 4]. By default, the antenna boresight direction is defined by the direction of the Sub-Satellite Point (SSP) and the point P is the position of the UT on the ground. The UT direction is identified by the (ϑ, φ) angles, where the boresight direction is (0,0). The direction cosines for the considered UT are derived as $u = \frac{P_y}{\|P\|} \sin\vartheta \sin\varphi$, and $v = \frac{P_z}{\|P\|} \cos\vartheta$. The total array response of the Uniform Planar Array (UPA) in the generic i-th UT direction (ϑ_i, φ_i) can be expressed as the Kronecker product of the array responses of two Uniform Linear Arrays (ULAs) lying on the y- and z-axis [14]. We first define the $1 \times N_H$ Steering Vector (SV) of the ULA along the y-axis $\mathbf{a}_H(\theta_i, \varphi_i)$ and the $1 \times N_V$ SV of the ULA along the z-axis $\mathbf{a}_V(\theta_i)$

$$\mathbf{a}_{\text{H}}(\vartheta_i,\varphi_i)= \left[1, e^{jk_0 d_{\text{H}} \sin\vartheta_i \sin\varphi_i}, \ldots, e^{jk_0 d_{\text{H}}(N_{\text{H}}-1)\sin\vartheta_i \sin\varphi_i}\right] \tag{1}$$

$$\mathbf{a}_{\text{V}}(\vartheta_i)= \left[1, e^{jk_0 d_{\text{V}} \cos\vartheta_i}, \ldots, e^{jk_0 d_{\text{V}}(N_{\text{V}}-1)\cos\vartheta_i}\right]. \tag{2}$$

where $k_0 = 2\pi\lambda$ is the wave number, N_{H}, N_{V} denote the number of array elements on the horizontal (y-axis) and vertical (z-axis) directions respectively with $N = N_{\text{H}} \cdot N_{\text{V}}$ and $d_{\text{H}}, d_{\text{V}}$ denote the distance between adjacent array elements on the y- and z-axis respectively. We assume that the array is equipped with directive antenna elements, whose radiation pattern is denoted by $g_E(\vartheta_i, \varphi_i)$. Finally, we can express the $(1 \times N)$ SV of the UPA at the satellite targeted for the i-th user as the Kronecker product of the 2 SVs along each axis multiplied by the element radiation pattern:

$$\mathbf{a}(\vartheta_i, \varphi_i) = g_E(\vartheta_i, \varphi_i)\, \mathbf{a}_{\text{H}}(\vartheta_i, \varphi_i) \otimes \mathbf{a}_{\text{V}}(\vartheta_i) \tag{3}$$

The CSI vector at feed level $\hat{\mathbf{h}}_i$ represents the channel between the N radiating elements and the generic i-th on-ground UT, with $i = 1, \ldots, K$, and can be written as:

$$\hat{\mathbf{h}}_i = G_i^{(rx)} \frac{\lambda}{4\pi d_i} \sqrt{\frac{L_i}{\kappa B T_i}} e^{-j\frac{2\pi}{\lambda} d_i} \mathbf{a}(\vartheta_i, \varphi_i) \tag{4}$$

in which, d_i is the slant range between the generic i-th user and the satellite, λ is the wavelength, $\kappa B T_i$ denotes the equivalent thermal noise power, with κ being the Boltzmann constant, B the user bandwidth (assumed to be the same for all users), and T_i the equivalent noise temperature of the i-th UT. $G_i^{(rx)}$ denotes the receiving antenna gain for the i-th UT, while L_i denotes all the additional losses per user, such as atmospheric, antenna, and cable losses. By collecting all of the K CSI vectors, it is possible to build a $K \times N$ complex channel matrix at system level $\hat{\mathbf{H}} = \left[\hat{\mathbf{h}}_1^\intercal, \hat{\mathbf{h}}_2^\intercal, \ldots, \hat{\mathbf{h}}_K^\intercal\right]^\intercal$, where the generic k-th row contains the CSI vector of the k-th user and the generic n-th column contains the channel coefficients from the n-th on-board feed towards the K on-ground users. Given the set of all users to be scheduled, denoted with $\mathcal{U} = \{U_1, U_2, \ldots, U_K\}$, the Radio Resource Management (RRM) algorithm defines a possible users' partitioning $\{\mathcal{C}_1, \mathcal{C}_2, \ldots, \mathcal{C}_P\}$ where $\mathcal{C}_p \subseteq \mathcal{U}$ is defined as cluster and $|\mathcal{C}_p| = K_p$ is defined as the cardinality of the p-th cluster with $p = 1, \ldots, P$. In order to minimize the the total number of clusters P, we further assume that each user can be assigned only to one cluster (as in [11, 9]), therefore clusters are disjoint sets of users, $\mathcal{C}_i \cap \mathcal{C}_j = \varnothing,\ \forall i, j$. In each time slot, users belonging to cluster $\mathcal{C}_p$ are selected, leading to a $K_p \times N$ complex scheduled channel matrix $\hat{\mathbf{H}}_p \subseteq \hat{\mathbf{H}}$, which contains only the rows of the scheduled users in the p-th cluster. The selected beamforming algorithm computes for each cluster a $N \times K_p$ complex beamforming matrix $\mathbf{W}_p = [\mathbf{w}_1^{(p)}, \mathbf{w}_2^{(p)}, \ldots, \mathbf{w}_{K_p}^{(p)}]$, where $\mathbf{w}_i^{(p)}$ denotes the $N \times 1$ beamformer designed for the i-th user in the p-th cluster. The matrix $\mathbf{W}_p$ projects the K_p dimensional column vector $\mathbf{s}_p = [s_1, s_2, \ldots, s_{K_p}]^\intercal$ containing the unit-variance users' symbols onto the N-dimensional space defined by the antenna feeds. Thus, in the feed space, the computation of the beamforming matrix allows for the generation of a dedicated beam towards each user direction. The signal received by the i-th user in the p-th cluster can be expressed as follows [9]

$$y_k^{(p)} = \mathbf{h}_k \mathbf{w}_k^{(p)} s_k + \sum_{\substack{i=1 \\ i \neq k}}^{K_p} \mathbf{h}_k \mathbf{w}_i^{(p)} s_i + z_k^{(p)} \tag{5}$$

The K_p-dimensional vector of received symbols in the p-th cluster is

$$\mathbf{y}_p = \mathbf{H}_p \mathbf{W}_p \mathbf{s}_p + \mathbf{z}_p \tag{6}$$

It shall be noted that the estimated channel matrix $\hat{\mathbf{H}}$ at time t_0 is used to compute the scheduling and the beamforming matrices $\mathbf{W}_p$ in the estimation phase, while the beamformed

symbols are sent to the users at a time instant $t_0+\Delta t$, in which the scheduled channel matrices and vectors are different and denoted as $\mathbf{H}_p$ and $\mathbf{h}_k$, respectively. The SINR for user k belonging to cluster p can be computed as

$$\text{SINR}_k^{(p)} = \frac{\left\|\mathbf{h}_k \mathbf{w}_k^{(p)}\right\|^2}{1 + \sum_{\substack{i=1 \\ i\neq k}}^{K_p} \left\|\mathbf{h}_k \mathbf{w}_i^{(p)}\right\|^2} \tag{7}$$

We can define the per-cluster sum-rate capacity as:

$$\Gamma_p = B \sum_{k=1}^{K_p} \log_2(1 + \text{SINR}_k^{(p)}) \tag{8}$$

where B denotes the bandwidth. Given that each user can be assigned to only one cluster and taking into account the duty cycle associated with each cluster in TDMA, we can define the throughput experienced by the k-th user as:

$$R_k = \frac{B}{P} \log_2 \left(1 + \text{SINR}_k^{(p)}\right) \tag{9}$$

The beamforming matrix $\mathbf{W}_p$, which is computed on a cluster basis, is based on the linear Minimum Mean Square Error (MMSE) equation:

$$\mathbf{W}_p = \hat{\mathbf{H}}_p^H (\hat{\mathbf{H}}_p \hat{\mathbf{H}}_p^H + \alpha \mathbf{I}_{K_p})^{-1} \tag{10}$$

where $\mathbf{I}_{K_p}$ indicates the $K_p \times K_p$ identity matrix and $\alpha = \frac{N}{P_t}$ is the regularisation factor with P_t the total on-board power. We consider the following two options for power normalization: Sum Power Constraint (SPC) and Maximum Power Constraint (MPC), which are defined as:

$$\widetilde{\mathbf{W}}_p^{(\text{SPC})} = \frac{\sqrt{P_t}\mathbf{W}_p}{\sqrt{\text{tr}(\mathbf{W}_p \mathbf{W}_p^H)}} \quad \widetilde{\mathbf{W}}_p^{(\text{MPC})} = \frac{\sqrt{P_t}\mathbf{W}_p}{\sqrt{N \max_j \left[\mathbf{W}_p \mathbf{W}_p^H\right]_{j,j}}} \tag{11}$$

3. USER SCHEDULING

We denote with $\mathcal{G} = (\mathcal{V}, \mathcal{E})$ an undirected and unweighted graph with vertex set $\mathcal{V}$ and edge set $\mathcal{E}$. A clique $\mathcal{Q}$ of $\mathcal{G}$ is a subset of the vertices, $\mathcal{Q} \subseteq \mathcal{V}$, such that every two distinct vertices are adjacent, i.e., $\mathcal{Q}$ is a complete subgraph. In our LEO NTN MIMO scenario, the set of vertices $\mathcal{V}$ coincides with the set of users $\mathcal{U}$ and the edge set is constructed based on the channel Coefficient of Correlation (CoC) [11, 12], defined as

$$[\mathbf{\Psi}]_{i,j} = \frac{\left|\mathbf{h}_i \mathbf{h}_j^H\right|}{\|\mathbf{h}_i\| \, \|\mathbf{h}_j\|} \tag{12}$$

where $[\mathbf{\Psi}]_{i,j} \in [0, 1]$. The set of edges $\mathcal{E}$ of the $\mathcal{G}$ graph is completely determined by its adjacency matrix $\mathbf{A}$, whose entries are defined as:

$$[\mathbf{A}]_{i,j} = \begin{cases} 1, & [\mathbf{\Psi}]_{i,j} \leq \delta_{th} \\ 0, & [\mathbf{\Psi}]_{i,j} > \delta_{th} \end{cases} \tag{13}$$

where δ_{th} denotes the graph threshold. An edge between U_i and U_j implies that their channels $\mathbf{h}_i$ and $\mathbf{h}_j$ are considered nearly orthogonal and therefore they can be co-scheduled. The graph threshold determines the density of the graph $D(\mathbf{\Psi}, \delta_{th})$ which can be computed as

$$D(\mathbf{\Psi}, \delta_{th}) = \frac{2|\mathcal{E}|}{|\mathcal{V}|\,(|\mathcal{V}| - 1)} = \frac{1}{2} \sum_{i=1}^{K} \sum_{j=1}^{K} [\mathbf{A}]_{i,j} \tag{14}$$

Algorithm 1 Improved Max Clique scheduler with constant graph density.

Require: Set of users $\mathcal{U}$, channel CoC matrix $\mathbf{\Psi}$ and target graph density ϵ_t
Initialize $p = 1$ and $K = |\mathcal{U}|$
while $\mathcal{U} \neq \varnothing$ **do**
  δ_{th} = BISECTIONMETHOD($\mathbf{\Psi}$, 0, 1, ϵ_t, tol, $I_{\max}$)
  Compute $\mathbf{A}$ as in (13)
  $\mathcal{Q}_{\max}$ = MAXCLIQUEDYN($\mathbf{A}$)
  $\mathcal{C}_p \leftarrow \mathcal{Q}_{\max}$ and $K_p \leftarrow |\mathcal{C}_p|$
  Remove all rows and columns of $\mathbf{\Psi}$ associated with users in $\mathcal{Q}_{\max}$
  $\mathcal{U} \leftarrow \mathcal{U} - \mathcal{Q}_{\max}$ and $K \leftarrow K - K_p$
  $p \leftarrow p + 1$
end while
procedure BISECTIONMETHOD($\mathbf{\Psi}$, a, b, ϵ_t, tol, $I_{\max}$)
  $c = \frac{a+b}{2}$ and $i = 0$
  while $|f(\mathbf{\Psi}, c)| > tol \;\&\; i < I_{\max}$ **do**
    if $f(\mathbf{\Psi}, b) \cdot f(\mathbf{\Psi}, c) < 0$ **then**
      $a = c$
    else
      $b = c$
    end if
    $c = \frac{a+b}{2}$
    $i \rightarrow i + 1$
  end while
  return c
end procedure

As illustrated in Alg. 1, we design a greedy iterative algorithm that aims at minimizing the total number of clusters P and maximizing the total sum-rate capacity. Similarly to [9], the iterative procedure searches for the maximum clique $\mathcal{Q}_{\max}$ in the graph through the efficient MaxCliqueDyn algorithm [15] and declares it as a cluster; at each step the nodes in $\mathcal{Q}_{\max}$ and any edges connected to them are removed. The main novelty in the new algorithm is how the graph is updated after each pruning. In [9], since a constant graph threshold value is set at the beginning of the procedure, only graph pruning is implemented at each step. Here instead we first set a constant target graph density value ϵ_t, then at each step (both at the beginning and after each pruning), we search for the threshold δ_{th} such that $D(\mathbf{\Psi}, \delta_{th}) = \epsilon_t$. To obtain the respective threshold value for the required target density ϵ_t, we aim at finding the root of the function $f(\mathbf{\Psi}, \delta_{th}) = D(\mathbf{\Psi}, \delta_{th}) - \epsilon_t$ through the bisection method [16]. Within this method, the root to be found is initially bounded between 0 and 1, the search interval is repeatedly halved until convergence is reached through the parameter tol. Finally, the parameter $I_{\max}$ limits iterations to prevent infinite loops.

Table 1: Simulation parameters.

Parameter	Value	Parameter	Value
Carrier frequency	2 GHz	Propagation scenario	Line of Sight
System band	S (30 MHz)	System scenario	urban
Beamforming space	feed	Total on-board power density, $P_{t,\text{dens}}$	4 dBW/MHz
Receiver type	VSAT	Coverage area	101077 km^2
Receiver antenna gain	39.7 dBi	User density	0.05 user/km^2
Noise figure	1.2 dB	Number of transmitters N	1024 (32×32 UPA)

4. SIMULATION SETUP AND RESULTS

In this section, we present the outcomes of the extensive numerical simulations with the parameters specified as in Tab. 1. The assessment is performed in full buffer conditions, i.e., infinite traffic demand. A single LEO satellite is considered at a distance of 600 Km from the earth. On average the total number of users are $K = 2850$. The user terminals are fixed VSAT and the propagation scenario is the line of sight (LOS) model based on TR 38.821 and TR 38.811 [17, 18]. In all simulations, the performance of the improved maximum (Max) clique-based algorithm with constant graph density is compared against our original Max clique scheduler and MADOC. Aiming at maximizing the total sum-rate capacity, we performed a heuristic optimization of the graph density for the improved Max clique, and we obtained optimized thresholds for the original Max clique and MADOC for both MMSE-SPC and MMSE-MPC as shown in Tab. 2. It is evident that the improved Max clique offers the highest average per-cluster sum-rate capacity (Gbps), and mean cluster size as compared to the other schedulers, with a very large improvements in both indicators w.r.t. the original Max clique.

Table 2: Simulation results for graph density optimization.

Parameters		Original Max clique	MADOC	Improved Max clique
Optimized threshold graph density	SPC	0.32	0.58	0.965
	MPC	0.27	0.51	0.957
Mean cluster size	SPC	46.37	56.34	59.42
	MPC	42.81	48.56	50.29
Sum-rate capacity (Gbps)	SPC	17.93	21.17	21.49
	MPC	15.82	18.19	18.64

In Fig. 1, the Cumulative Distribution Function (CDF) of the per-cluster sum-rate capacity for all the considered schedulers is shown. Only 8% of the clusters experience less than 15 Gbps with the improved Max clique for MMSE-SPC, whereas the percentage increases to 28% with the original max clique. Fig. 2 shows the CDF of the users' throughput. It can be noticed that on average the throughput with the improved Max clique with MMSE-SPC is increased by 0.2 Mbps w.r.t. MADOC, and 1.4 Mbps w.r.t. the original Max clique. To further validate the results, Fig. 3 shows the histograms of the cluster size distributions for the improved and the original Max clique schedulers. It is clear that Fig. 3b shows a significant reduction in the cluster size variance, as opposed to Fig. 3a.

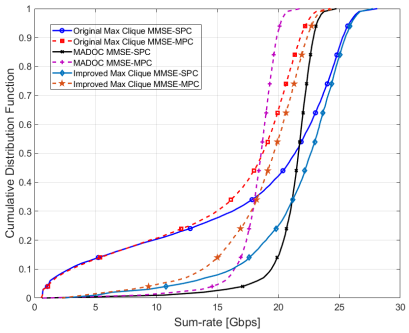

Fig. 1: CDF of the per-cluster sum-rate capacity.

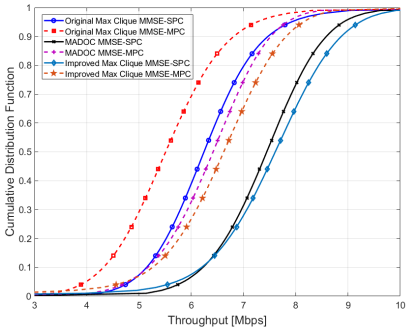

Fig. 2: CDF of the user throughput.

5. CONCLUSION

In this paper, we addressed the problem of user scheduling for LEO MU-MIMO NTN systems by proposing a low-complexity graph-based iterative procedure with constant graph density with the goal of maximizing the per-cluster sum-rate capacity. Results show that the proposed algorithm significantly improves the sum-rate capacity, offers higher throughput, and allows to significantly reduce the variance of the cluster size distribution w.r.t. [9], thus improving the fairness among users and the overall performance.

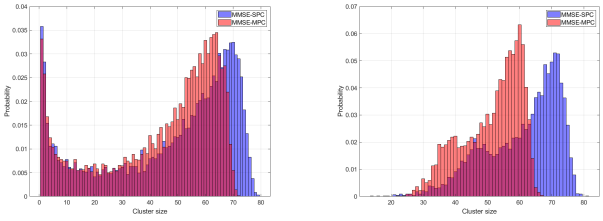

(a) Original Max Clique. (b) Improved Max Clique.

Fig. 3: Cluster size distribution for both original and improved Max clique schedulers.

6. REFERENCES

[1] Alessandro Guidotti and Alessandro Vanelli-Coralli, "Clustering strategies for multicast precoding in multi-beam satellite systems," *International Journal of Satellite Communications and Networking*, vol. 38, no. 2, pp. 85–104, 2020.

[2] Alessandro Guidotti and Alessandro Vanelli-Coralli, "Geographical scheduling for multicast precoding in multi-beam satellite systems," in *2018 9th Advanced Satellite Multimedia Systems Conference and the 15th Signal Processing for Space Communications Workshop (ASMS/SPSC)*, 2018, pp. 1–8.

[3] Hanan Weingarten, Yossef Steinberg, and Shlomo Shitz Shamai, "The capacity region of the gaussian multiple-input multiple-output broadcast channel," *IEEE transactions on information theory*, vol. 52, no. 9, pp. 3936–3964, 2006.

[4] M. Rabih Dakkak, Daniel Gaetano Riviello, Alessandro Guidotti, and Alessandro Vanelli-Coralli, "Evaluation of MU-MIMO digital beamforming algorithms in B5G/6G LEO satellite systems," in *2022 11th Advanced Satellite Multimedia Systems Conference and the 17th Signal Processing for Space Communications Workshop (ASMS/SPSC)*, 2022, pp. 1–8.

[5] Miguel Ángel Vázouez, Xavier Artiga, and Ana I. Pérez-Neira, "Closed-form multicast precoding for satellite flexible payloads," in *2021 29th European Signal Processing Conference (EUSIPCO)*, 2021, pp. 910–914.

[6] Alessandro Guidotti and Alessandro Vanelli-Coralli, "Design trade-off analysis of precoding multi-beam satellite communication systems," in *2021 IEEE Aerospace Conference (50100)*, 2021, pp. 1–12.

[7] Pantelis-Daniel Arapoglou, Konstantinos Liolis, Massimo Bertinelli, Athanasios Panagopoulos, Panayotis Cottis, and Riccardo De Gaudenzi, "MIMO over satellite: A review," *IEEE Communications Surveys & Tutorials*, vol. 13, no. 1, pp. 27–51, 2011.

[8] J. Tronc, P. Angeletti, N. Song, M. Haardt, J. Arendt, and G. Gallinaro, "Overview and comparison of on-ground and on-board beamforming techniques in mobile satellite service applications," *International Journal of Satellite Communications and Networking*, vol. 32, no. 4, pp. 291–308, 2014.

[9] Daniel Gaetano Riviello, Bilal Ahmad, Alessandro Guidotti, and Alessandro Vanelli-Coralli, "Joint graph-based user scheduling and beamforming in LEO-MIMO satellite communication systems," in *2022 11th Advanced Satellite Multimedia Systems Conference and the 17th Signal Processing for Space Communications Workshop (ASMS/SPSC)*, 2022, pp. 1–8.

[10] Xinping Yi and Edward K. S. Au, "User scheduling for heterogeneous multiuser MIMO systems: A subspace viewpoint," *IEEE Transactions on Vehicular Technology*, vol. 60, no. 8, pp. 4004–4013, 2011.

[11] Kai-Uwe Storek and Andreas Knopp, "Fair user grouping for multibeam satellites with MU-MIMO precoding," in *GLOBECOM 2017 - 2017 IEEE Global Communications Conference*, 2017, pp. 1–7.

[12] Eduardo Castañeda, Adão Silva, Atílio Gameiro, and Marios Kountouris, "An overview on resource allocation techniques for multi-user MIMO systems," *IEEE Communications Surveys & Tutorials*, vol. 19, no. 1, pp. 239–284, 2017.

[13] Alessandro Guidotti, Carla Amatetti, Fabrice Arnal, Baptiste Chamaillard, and Alessandro Vanelli-Coralli, "Location-assisted precoding in 5G LEO systems: architectures and performances," in *2022 Joint European Conference on Networks and Communications & 6G Summit (EuCNC/6G Summit)*, 2022, pp. 154–159.

[14] Giusi Alfano, Carla-Fabiana Chiasserini, Alessandro Nordio, and Daniel Gaetano Riviello, "A random matrix model for mmWave MIMO systems," *Acta Physica Polonica B*, vol. 51, pp. 1627, 01 2020.

[15] Janez Konc and Dusanka Janezic, "An improved branch and bound algorithm for the maximum clique problem," *MATCH Commun. Math. Comput. Chem.*, vol. 58, no. 3, pp. 569–590, 2007.

[16] Richard L. Burden and J. Douglas Faires, *Numerical Analysis*, Cengage Learning, 10th edition, 2015.

[17] 3GPP, "Solutions for NR to support non-terrestrial networks (NTN) (release 16)," Rec. TR 38.821 V16.1.0, 3GPP, May 2021.

[18] 3GPP, "Service requirements for the 5G system; stage 1 (release 18)," Tech. Rep. TS 22.261 V18.2.0, 3GPP, Mar. 2021.